Excimer laser fabrication of polymer microfluidic devices

Joohan Kim and Xianfan Xu[a)]
School of Mechanical Engineering, Purdue University, West Lafayette, Indiana 47907

(Received 15 May 2002; accepted 10 February 2003)

Silicon has been a primary material for fabrication of microelectromechanical systems (microfluidic devices in MEMS) for several decades. This is due to the fact that the MEMS techniques were derived from those used for microfabrication in the semiconductor industry. These techniques are well developed, and can be readily applied for silicon based MEMS fabrication. Nowadays, alternative manufacturing materials and techniques are needed for reducing costs and meeting new requirements. Polymers have many advantages because of their low costs and applications in microfluidics. This article describes processes for fabricating polymer-based MEMS, including machining and bonding techniques. Microfluidic parts are machined on polymers with a KrF excimer laser ($\lambda = 248$ nm). Mask patterning and direct laser writing techniques are used. A silicon-on-glass process and an infrared laser bonding process are applied to assemble the machined parts with transparent cover glasses or plastics. As an example, a polymer micropump is fabricated and tested. It is shown that with the use of polymer materials, the performance of the pump is greatly improved. © *2003 Laser Institute of America.*

I. INTRODUCTION

The development of microelectromechanical systems (MEMS) has been driven by the need for miniaturization and lowering the overall manufacturing cost. Lasers have been widely used as a versatile manufacturing tool for decades and recently, research has been carried out on laser based MEMS fabrication.[1] The laser fabrication technique is fast, clean, safe, and convenient compared with chemical etching or deposition processes. Many traditional MEMS technologies are based on batch processes stemmed from the microelectronic industry. However, one of its disadvantages is its slow response to changing designs.[2] On the other hand, it is relatively easy to change laser processing conditions for different requirements; thus the laser technique is also a suitable tool for rapid prototyping.[3]

Miniaturized bio-MEMS devices have many applications cultivated by the developments of MEMS technology in fields such as clinical diagnostics and drug development.[4] The laser ablation technique can be applied to fabricate bio-MEMS components such as reservoirs and complex connecting channels on polymers, which can be used in DNA sequencing and enzyme assays. Properly designed microchannels provide efficient mixing of enzyme and substrate for these processes.[5] Diagnostic devices also make use of microfluidic channels and microfilter arrays for performing bioprocessing functions. He *et al.* developed a microchromatography system with the functions of traditional columns packed with particles.[6] Microfabricated column structures were used as microfilters: microchannels with dimensions from less than 1 μm to tens of microns can block specific types of substances for bioseparation applications.[7]

This article addresses ultraviolet (UV) excimer laser ablation of polymers for fabrication of microstructures used in microfluidic devices. Since the demonstration of UV laser ablation of polymers some 20 yr ago,[8] much research has been conducted to investigate the process of laser ablation of polymers. The photochemical bond-breaking theory[9–11] and the thermal reaction theory[12,13] have been introduced to explain the ablation mechanism. The former proposes that UV irradiation produces radicals at the polymer surface which can react with molecules from the original polymer surface or surrounding molecules and generate volatile molecules such as CO and CO_2, causing ablation on the surface.[14,15] The latter states that the intensive local heating induces an explosive pyrolysis which leads to the material ablation process.[16] A generally accepted theory involves both photochemical and thermal processes.[17]

Several approaches of applying the UV laser ablation technique for direct or indirect fabrication of microstructures have been attempted and reported.[18–20] In this article, we will demonstrate UV laser ablation and bonding techniques of polymers for fabrications of microfluidic devices. Mask patterning and direct laser writing techniques are used for making various types of fluidic channels and reservoirs. The spin-on glass (SOG) process and the infrared (IR) laser bonding process are tested for assembly operations. As an example, a polymer micropump is fabricated and tested.

II. LASER ABLATION

A KrF excimer laser ($\lambda = 248$ nm) is used as a laser source to ablate polymers. An optical imaging system, LightBench (Resonetics, Inc.) with a three-element processing lens ($f = 88.4$ mm) forms 5–10× demagnified images on the polymer surface. Laser fluences of 0.1–3.0 J/cm^2 and repeti-

a)Author to whom correspondence should be addressed; electronic mail: xxu@ecn.purdue.edu

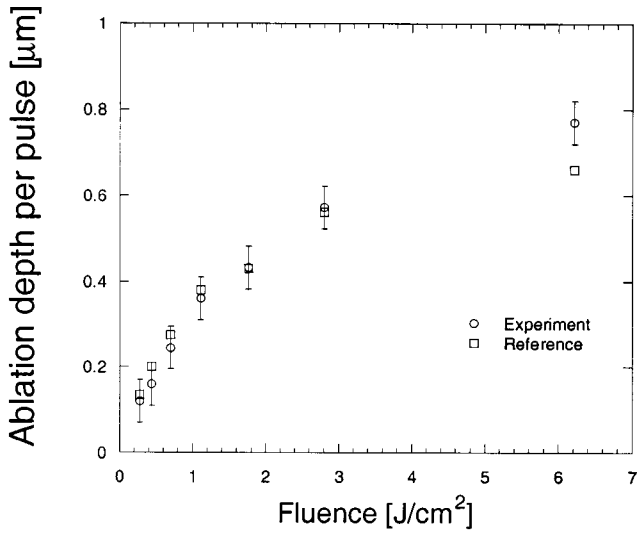

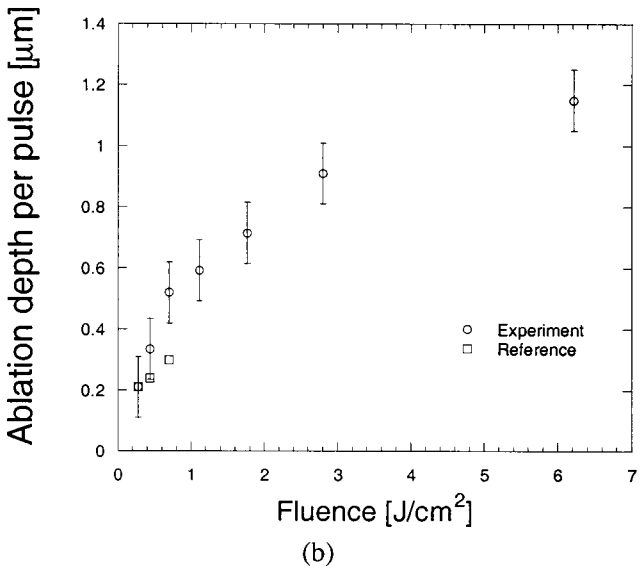

FIG. 1. Ablation depth per pulse vs fluence: (a) Kapton and (b) PET. Reference data are taken from Refs. 21 and 22, respectively.

tion rates of 1–8 Hz are used. Various masks, including a slit of 220 μm wide and pin holes of diameters 200 and 600 μm are employed. Polyethyleneterephthalate (PET) and polyimide (Kapton) films with a thickness of 100 μm and acrylic with a thickness of 3 mm are used as base materials. The motion stages have a 0.1 μm resolution, and their moving speed varies between 1 and 10 μm/s. A charge coupled device camera is installed on the LightBench to monitor the ablation process.

Ablation depths of the target materials as a function of laser fluence are measured. Figure 1 shows the ablated depths of Kapton and PET. These values are obtained using a single laser pulse. It is seen that the results obtained in this work are close to those reported in the literature.[21,22] Ablation per laser pulse from multiple pulses or overlapping pulses can be different since the fluence at the machined surface can be changed due to the divergence of the laser beam. From the Beer's Law and data of the ablation depth in the low laser fluence range, the threshold fluences for Kapton

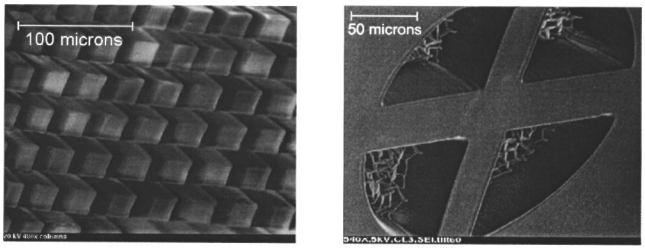

FIG. 2. Scanning electron microscope (SEM) photographs of: (a) microcolumns and (b) a cross-shape wall in a circle.

and PET ablation are found to be around 0.07 and 0.1 J/cm^2, respectively. These values are higher than those from the literature[16,23] and the discrepancies are thought to come from less data points at low fluences ($<$1 J/cm^2). The experimental data are in good agreement with the Beer's absorption law in the fluence range between 0.2 and 1.0 J/cm^2. However, in the range of high fluences (above 1.8 J/cm^2), the measured ablation rate begins to level off. This is due to the strong shielding effect of the laser ejected plume at high laser fluences.[21]

The side walls of the excimer laser ablated polymer structures are usually tapered and the angle varies with the laser pulse parameters and material properties. The main reason is that, as the ablation depth increases, the wave front has different intensity distribution. Moreover, the tapered wall structure leads to significant attenuation of the fluence.[24] Using a proper laser fluence (usually high fluence) can reduce the angle of taper.[25] In order to predict the shape of the walls of the micromachined structures, a model based on a local distribution of a beam in the developing structure has been described.[26] In this work, high laser fluences are used for fabricating channels with straight walls.

A. Mask patterning

Mask patterning is very similar to lithography. A laser beam passes through a mask with a prefabricated pattern and irradiates on the polymer surface by an imaging lens set. In our system, the ablated patterns are reduced images with demagnification of around ten. Results of mask patterning, such as a rectangular channel and a circle with a cross in PET, are shown in Fig. 2. Figure 2(a) shows microcolumns whose side is less than 20 μm. A slit of 5 mm long and 200 μm wide was employed to produce a slot image, and arrays of slots were imaged in perpendicular directions to fabricate the column array. This array of columns can be used as a microfilter in a fluid separation device.

A cross-shaped wall in a circular hole is shown in Fig. 2(b). Nap type patterns on the bottom of PET are obtained. The nap structure formation on PET has been reported in several articles.[27,28] This nap structure may assist mixing of fluids in microfluidic devices. However, it is not preferable in most applications. Moving the target during laser ablation can reduce these patterns drastically. It is also suggested that a well defined pattern can be obtained if a stopping layer such as a Ti film is applied on the back side of the polymer.[29]

The characteristics of the mask projection method can be summarized as: (1) complex patterns can be machined with

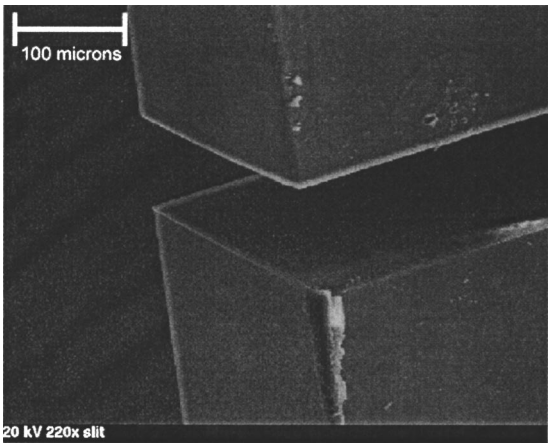

FIG. 3. SEM photograph of an excimer laser machined microchannel in PET.

the use of a mask and (2) batch production is possible with an array of the same patterns on the mask.

B. Direct laser writing

The other technique for fabricating microstructures is direct laser writing—patterns are created by moving the target using computer controlled stages. In this work, the image on the target surface has a rectangular shape with a dimension of 20×40 μm, a square shape of 20×20 μm, or a circular shape with a diameter of 20–60 μm. The computer controlled stages follow predesigned paths to produce various types of patterns on the polymer surfaces. The removal rate can be precisely controlled from the number of laser pulses. However, to make a smooth pattern, a high pulse repetition rate and a low scanning velocity are usually necessary. Unlike mechanical machining, making a blank channel with moving stages generates tapered geometries at the two ends of the channel because those places are not irradiated by the same number of laser pulses compared with the middle part of the channel as the stage moves.

Figure 3 shows a through channel in PET with smooth walls and clean edges. It has been observed that at a low fluence, the wall taper angle is around 3°–10°. However at high fluences, a reversed taper (undercut) can be produced.[26] In order to make a straight wall, the fluence has to be controlled within a proper level. In the case of the through channel shown in Fig. 3, a fluence of 3 J/cm^2 was used which is higher than the normal fluence level for the polymer ablation process (typically $<$0.5 J/cm^2). Figure 4(a) is a simple but typical microfluidic device: a single microchannel with reservoirs. The channel was ablated by scanning a 20 μm by 20 μm square image and the reservoirs were ablated using mask patterning. Figure 4(b) shows a cross-shaped microchannel with two reservoirs, which is a structure typical of chromatography used for enzyme assays performed by combining chemicals at the cross junction and allowing them to diffusively mix in a reaction channel.[5]

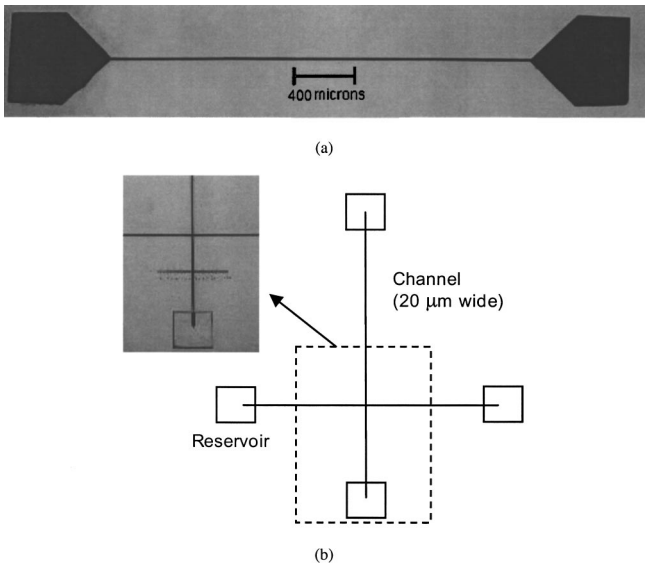

FIG. 4. (a) Fluidic channel of 20 μm wide with two reservoirs and (b) cross-shape channel and reservoirs.

III. BONDING TECHNIQUES

The laser machined polymers need to be bonded with another film or plate such as glass or polymer to be used in a microfluidic device. Transparent covers are often useful for optical measurements. If a heating procedure is necessary during the bonding process, the operating temperature must not exceed the softening or melting temperature of the polymers. As such, some traditional bonding techniques for MEMS fabrication are not applicable to polymers due to the high operation temperatures. In addition, there are several other requirements for bonding microstructures. The bonding adhesive layer, if it is used, must be very thin. This is because the ablated depth of the microstructures can be as small as a few microns, so it is possible to fill up the microstructures when a thick layer of adhesive is applied. Therefore, the viscosity of adhesive materials must be very low (less than 200 cps). Two bonding techniques, SOG and IR laser bonding, are applied in this work and are described as follows.

A. Spin-on glass bonding

The SOG process was originally developed in the microelectronics industry for deposition of silicon oxide during planarization processes and fabrication of silicon-on-insulator structures due to good crystallinity on the silicon surface.[30,31] Yamada *et al.* reported using SOG for bonding silicon wafer and silicon nitride.[32] Much research has been carried out to apply SOG as an adhesive substance for silicon wafers.[33] The procedure of SOG bonding used in this work is as follows. First, the cover such as a glass slide is cleaned with acetone or methanol. Second, the SOG layer was spun on the glass slide at 2000 rpm for 40 s. The thickness of the spin coated SOG layer at 2000 rpm was in the range of 490–500 nm. The machined polymer plate or film is then placed on top of the glass and both parts are cured for 120 min at 200 °C. Kapton films can be used in SOG bonding since the melting temperature of Kapton is 230 °C. Figure 5

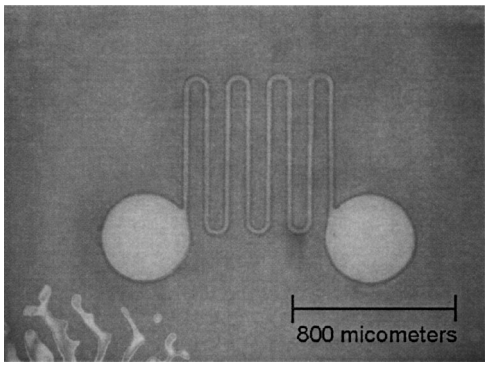

FIG. 5. SOG bonding sample (Kapton film on a glass substrate).

shows the top view of a bonded sample, which is used in a microscale heat exchanger. The Kapton film is completely bonded to the glass substrate.

B. IR laser bonding

The bonding processes using adhesives may not be applicable when high optical transmission in the bonding zone is needed or the melting temperature of the polymer is below 200 °C. Also, release vapors in the hardened adhesives could be difficult to control in the joining zone.[34] Laser techniques have been recently developed to bond polymers.[35,36] The schematic diagram of this process is shown in Fig. 6. The parts to be bonded consist of a transparent polymer and an opaque one. The laser beam passes through the transparent part and is absorbed by the opaque part. Heat is conducted into the transparent part and the bonding process occurs at the interface due to melting and resolidification. The experimental setup used in this work consists of a laser source, an aperture, a lens, and a target holder. A cw fiber laser ($\lambda = 1100$ nm) is focused on the bonding area with the use of a lens which has a 200 mm focal length. An aperture is used for reducing the laser energy to a proper level. Materials are acrylics: one being clear and the other being opaque. The processing parameters are summarized in Table I.

Too low laser power can lead to a failure of adhesion and too high power will cause generation of bubbles at the interface or even burning of the materials. The quality of laser bonding can be evaluated with several aspects such as the strength of the joining part, optical properties at the interface, and the presence of air bubbles, which are determined by the transient temperature distribution at the bonding zone. The

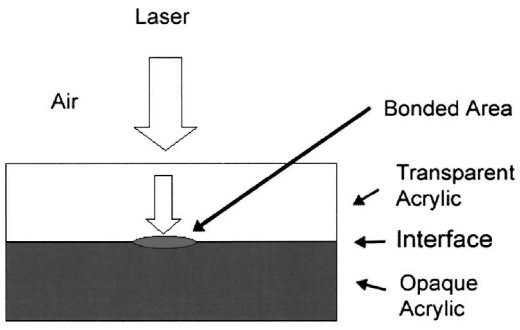

FIG. 6. Schematic diagram of laser bonding.

TABLE I. Parameters of IR laser bonding.

Power	29.5 mW
Focused laser beam diameter	0.3 mm
Power intensity	0.42 W/mm^2
Aperture diameter	up to 4 mm
Focal length of the lens	200 mm
Target position from the lens	240 mm
Exposure time	1–60 s

temperature distribution is related to the amount of radiation energy absorbed at the opaque surface and the conduction process in the materials, and can be calculated using a thermal model. Assuming a perfect contact between the plates (no air gap), the temperature distribution in the material can be obtained from solving the following one-dimensional heat conduction equation

$$\rho c_p \frac{\partial T}{\partial t} = \frac{\partial}{\partial x}\left(k \frac{\partial T}{\partial x} \right), \tag{1}$$

where ρ is the density, c_p is the specific heat, k is the conductivity, and T is the temperature. The laser intensity input can be considered as a boundary condition at the interface as

$$-k_1 \cdot \frac{\partial T_1}{\partial x} = -k_2 \cdot \frac{\partial T_2}{\partial x} + q'', \quad \text{at } x = 0. \tag{2}$$

q is the laser power density absorbed at the interface which can be evaluated quantitatively with absorptivity, transmissivity, and reflectivity measurements. T_1 and T_2 are temperatures in two polymer layers. The refractive index of the transparent plate was found to be $1.45 - i\ 1.51 \times 10^{-6}$, and the reflective index of opaque one is $1.45 - i\ 1.88 \times 10^{-1}$. Using these values, it is found that 87.52% of incident laser beam energy is absorbed at the interface.

The solution to the heat conduction equations, Eqs. (1) and (2), can be expressed as[37]

$$T(x,t) - T_i = \frac{q''(\alpha t/\pi)^{1/2}}{k} \exp\left(\frac{-x^2}{4\alpha t} \right) - \frac{q'' x}{2k} \operatorname{erfc}\left(\frac{x}{2\sqrt{\alpha t}} \right), \tag{3}$$

where α is the thermal diffusivity and T_i is the initial temperature. The calculated transient temperature profile at various locations is shown in Fig. 7. The laser power intensity is 0.42 W/mm^2. In Fig. 7, the data above 110 °C have no significant meaning because the latent heat of phase change is not considered in the calculation and the material properties such as reflectivity, transmissivity, and diffusivity are significantly different from the values of the solid.

Figure 8(a) shows a laser bonded sample, where 3 s of exposure time was used and high quality bonding was achieved. As shown in Fig. 7, it can be deduced that the calculated temperature of the interface at this time is around 100 °C, which is near the melting temperature (105 °C). Therefore, the results with 3 s of the exposure time are in agreement with the calculated ones, and it can be concluded that high quality bonding can be obtained around the melting temperature. In the experiments, the level of deformation in-

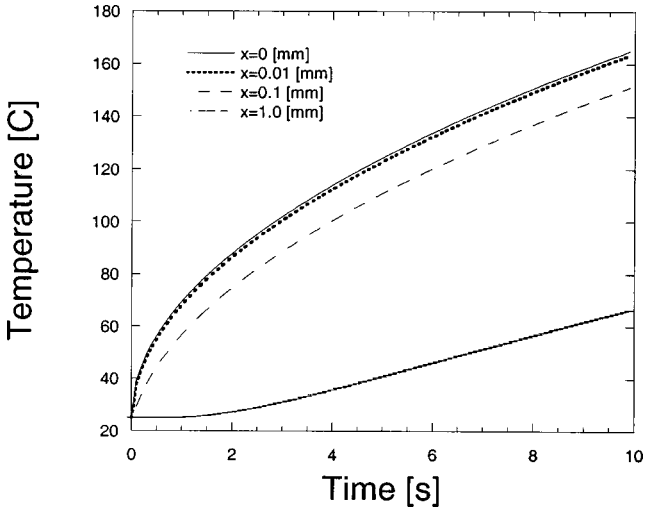

FIG. 7. Temperature profile on the opaque side at a laser power intensity of 0.42 W/mm^2.

creases as the heating time increases. When the laser heating time exceeds 60 s, bubbles at the interface can be observed.

The bonded spot size changes with parameters such as the laser beam diameter, the exposure time, and the laser intensity. If the sample is moved on a stage during laser irradiation, the laser bonded area can have a line shape or more complex shapes. Figure 8(b) shows a bonded sample which is rotated along a circle with a diameter of 5 mm during bonding. The bonded area has a width of 4 mm and is shown as the dark ring in the figure.

Comparing SOG bonding versus IR laser bonding, SOG bonding showed stronger adhesion at the interface compared with IR bonding, however the rate of successful bonding in the experiments was low: around 25%. This is due to the fact that the very thin bonding layer applied to very smooth surfaces such as wafers can be disturbed by the relatively rough surface of polymer materials. On the other hand, it is technically hard to apply a thin layer on patterned surfaces with the spin coating process. In this case, the bonding layer is not uniform and there is also the possibility of filling up the laser-fabricated patterns with the bonding material, which usually leads to blockage of the microchannels. In contrast, IR bonding has a potential in local bonding. However, the parameters must be chosen carefully to avoid deformation at the interface and to improve the bonding strength. Extensive

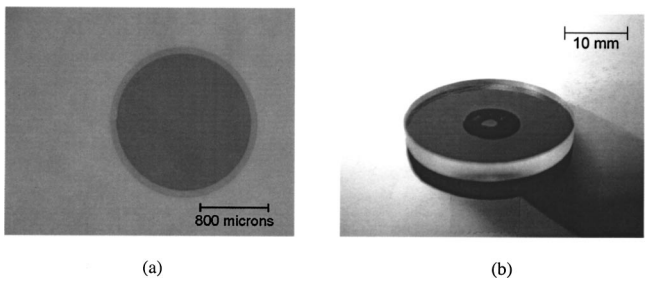

FIG. 8. Photograph of laser bonded samples: (a) a top view of a bonded spot and (b) circular bonding.

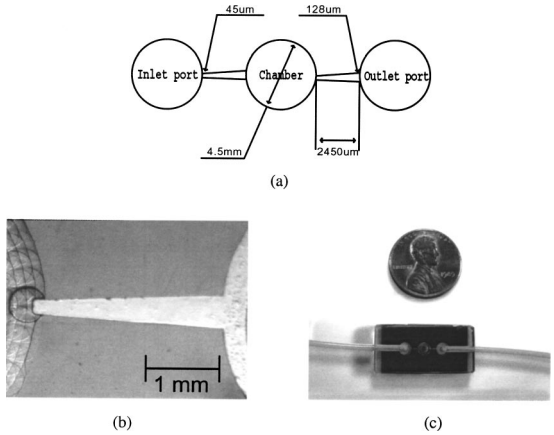

FIG. 9. (a) Schematic of the pump in a top view, (b) the laser fabricated diffuser of the pump, and (c) the assembled pump.

experimental tests, with the aid of the heat transfer model described above, are necessary to further improve the IR bonding technique.

IV. EXAMPLE OF A LASER-MACHINED MICROSYSTEM: A DIFFUSION MICROPUMP

Fabrication of microscale diffusion pumps has been reported in the literature,[38,39] using silicon as the base materials and employing standard lithography techniques. The schematic diagram of a diffusion micropump is shown in Fig. 9(a). It has an inlet diffuser, an outlet diffuser, and a diaphragm. As the diaphragm of the chamber is deformed downward by an actuator, more fluid flows out through the outlet nozzle and as it is deformed upward, more fluid enters through the inlet diffuser. Due to the different flow rates, a net flow from the inlet diffuser to the outlet diffuser can be induced. This type of diffusion pump has many advantages. For example, the valveless operation makes it simple and reliable.

In this work, Kapton is used as the base material and is machined by excimer laser ablation. It is expected that the polymer will allow a larger displacement of the diaphragm, resulting in higher efficiency. As shown in Fig. 9(b), the inlet channel, the outlet channel, and the chamber are machined by laser ablation. The neck of the diffuser channel and the diffuser length are around 45 and 2450 μm, respectively. The diameter of the chamber, which is covered with another Kapton layer, is 4.5 mm. Bonding with sufficient strength is necessary because the assembled system is subjected to high pressure liquid. Since SOG bonding shows a stronger bond compared with IR bonding, it is used here for bonding a glass substrate with a machined polymer film. The assembled system is shown in Fig. 9(c). For the purpose of testing, a pneumatic system is used to actuate the micropump. This system uses pulsations of high pressure air to actuate the diaphragm. The observed flow rate at a frequency of 15 Hz is around 11.5 mm^3/min. It is also expected that higher flow rates can be obtained if the diaphragm is actuated at higher frequencies using a different actuation method such as electrostatic actuation.

V. CONCLUSIONS

Laser techniques for fabricating microfluidic devices using polymer as the base material were presented. The mask patterning method is simple and rapid to fabricate repeated microstructures. Thus, it has advantages for batch production and fast patterning. On the other hand, direct laser writing with computer controlled moving stages can provide rapid changes of patterns. The combination of these two techniques can be used as a versatile tool for fabricating various microdevices on polymers. Techniques for bonding polymers were also studied. The SOG process led to a tight bonding of glass and polymer, and IR laser bonding can be used for microbonding on local areas of MEMS devices. A diffuser micropump was fabricated as a demonstration of laser fabrication of polymer based microsystems.

ACKNOWLEDGMENT

This work is supported by the Integrated Detection of Hazardous Materials (IDHM) Program, a Department of Defense project managed jointly by Center for Sensing Science and Technology, Purdue University, and Naval Surface Warfare Center, Crane, Indiana.

[1] A. S. Holmes and S. M. Saidam, ''Sacrificial layer process with laser-driven release for batch assembly operations,'' J. Microelectromech. Syst. **7**, 416–422 (1998).
[2] M. Lapczyna and M. Stuke, ''Rapid prototype fabrication of smooth microreactor channel systems in PMMA by VUV laser ablation at 157 nm for applications in genome analysis and biotechnology,'' Mater. Res. Soc. Symp. Proc. **526**, 143–148 (1998).
[3] R. Vaidya, L. M. Tender, G. Bradley, M. J. O'Brien II, M. Cone, and G. P. Lopez, ''Computer-controlled laser ablation: a convenient and versatile tool for micropatterning biofunctional synthetic surfaces for applications in biosensing and tissue engineering,'' Biotechnol. Prog. **14**, 371–377 (1998).
[4] M. S. Talary, J. P. H. Burt, N. H. Rizvi, P. T. Rumsby, and R. Pethig, ''Microfabrication of biofactory-on-a-chip devices using laser ablation technology,'' Proc. SPIE **3680**, 572–580 (1999).
[5] S. A. Zugel, B. J. Burke, F. E. Regnier, and F. E. Lytle, ''Electrophoretically mediated microanalysis of leucine aminopeptidase using two-photon excited fluorescence detection on a microchip,'' Anal. Chem. **72**, 5731–5735 (2000).
[6] B. He, N. Tait, and F. Regnier, ''Fabrication of nanocolums for liquid chromatography,'' Anal. Chem. **70**, 3790–3797 (1998).
[7] B. He, L. Tan, and F. Regnier, ''Microfabricated filters for microfluidic analytical systems,'' Anal. Chem. **71**, 1464–1468 (1999).
[8] R. Srinivasan and V. Mayne-Banton, ''Self-developing photoetching of poly(ethylene terephthalate) films by far-ultraviolet excimer laser radiation,'' Appl. Phys. Lett. **41**, 576–578 (1982).
[9] R. Srinivasan and B. Braren, ''Ultraviolet laser ablation of organic polymers,'' Chem. Rev. **89**, 1303–1316 (1989).
[10] G. D. Mahan, H. S. Cole, Y. S. Liu, and H. R. Philipp, ''Theory of polymer ablation,'' Appl. Phys. Lett. **53**, 2377–2379 (1988).
[11] E. Sutcliffe and R. Srinivasan, ''Dynamics of UV laser ablation of organic polymer surfaces,'' J. Appl. Phys. **60**, 3315–3322 (1986).
[12] J. E. Andrew, P. E. Dyer, D. Forster, and P. H. Key, ''Direct etching of polymer materials using a XeCl Laser,'' Appl. Phys. Lett. **43**, 717–719 (1983).
[13] B. Hopp, M. Csete, K. Revesz, J. Vinko, and Zs. Bor, ''Formation of the surface structure of polyethylene-terephtalate (PTE) due to ArF excimer laser ablation,'' Appl. Surf. Sci. **96–98**, 611–616 (1996).
[14] S. Lazare and R. Srinivasan, ''Surface properties of poly(ethylene terephthalate) films modified by far-ultraviolet radiation at 193 nm (laser) and 185 nm (low intensity),'' J. Phys. Chem. **90**, 2124–2131 (1986).
[15] D. Praschak, T. Bahners, and E. Schollmeyer, ''PET surface modifications by treatment with monochromatic excimer UV lamps,'' Appl. Phys. A: Mater. Sci. Process. **66**, 69–75 (1998).
[16] J. H. Brannon, J. R. Lankard, A. I. Baise, F. Burns, and J. Kaufman, ''Excimer laser etching of polymers,'' J. Appl. Phys. **58**, 2036–2043 (1985).
[17] H. Watanabe and M. Yamamoto, ''Laser ablation of poly(ethylene terephthalate),'' J. Appl. Polym. Sci. **64**, 1203–1209 (1997).
[18] F. Wagner and P. Hoffmann, ''Novel structure formation in poly(ethylene therephthalate) by scanning excimer laser ablation,'' Appl. Surf. Sci. **154–155**, 627–632 (2000).
[19] J. P. Rossier, P. Bercier, A. Schwarz, S. Loridant, and H. H. Girault, ''Topography, crystallinity and wettability of photoablated PET surfaces,'' Langmuir **15**, 5173–5178 (1999).
[20] W. Pfleging, T. Hanemann, W. Bernauer, and M. Torge, ''Laser micromachining of mold inserts for replication techniques—state of the art and applications,'' Proc. SPIE **4274**, 331–345 (2001).
[21] G. H. Pettit and R. Sauerbrey, ''Pulsed ultraviolet laser ablation,'' Appl. Phys. A: Solids Surf. **56**, 51–63 (1993).
[22] E. C. Harvey, T. R. Mackin, B. C. Dempster, and R. E. Scholten, ''Micro-optical structures for atom lithography studies,'' Proc. SPIE **3892**, 266–273 (1999).
[23] S. Lazare and P. Benet, ''Surface amorphization of Mylar films with the excimer laser radiation above and below ablation threshold: ellipsometric measurements,'' J. Appl. Phys. **74**, 4953–4957 (1993).
[24] S. Lazare, J. Lopez, and F. Weisbuch, ''High-aspect-ratio microdrilling in polymeric materials with intense KrF laser radiation,'' Appl. Phys. A: Mater. Sci. Process. **69**, S1–S6 (1999).
[25] T. W. Hodapp and P. R. Fleming, ''Modeling topology formation during laser ablation,'' J. Appl. Phys. **84**, 577–583 (1998).
[26] C. Paterson, A. S. Holmes, and R. W. Smith, ''Excimer laser ablation of microstructures: a numerical model,'' J. Appl. Phys. **86**, 6538–6546 (1999).
[27] E. Arenholz, V. Svorcik, T. Kefer, J. Heitz, and D. Bauerle, ''Structure formation in UV-laser ablated poly-ethylene-terephthalate (PET),'' Appl. Phys. A: Solids Surf. **53**, 330–331 (1991).
[28] F. Wagner and P. Hoffmann, ''Structure formation in excimer laser ablation of stretched poly(ethylene therephthalate) (PET): the influence of scanning ablation,'' Appl. Phys. A: Mater. Sci. Process. **69**, S841–S844 (1999).
[29] T. Klotzbucher, T. Braune, S. Sigloch, J. Hoßfeld, M. Neumeier, H. Bauer, and W. Ehrfeld, ''Polymer microsystems by excimer laser ablation: from rapid prototyping to large number fabrication,'' Proc. SPIE **4274**, 307–315 (2001).
[30] H. J. Quenzer, C. Dell, and B. Wagner, ''Silicon–silicon anodic-bonding with intermediate glass layers using spin-on glasses,'' Proceedings IEEE Micro Electro Mechanical Systems, San Diego, CA, 1996, pp. 272–276.
[31] A. Yamada, T. Kawasaki, and M. Kawashima, ''SOI by wafer bonding with spin-on glass as adhesive,'' Electron. Lett. **23**, 39–40 (1987).
[32] A. Yamada, T. Kawasaki, and M. Kawashima, ''Bonding silicon wafer to silicon nitride with spin-on glass as adhesive,'' Electron. Lett. **23**, 314–315 (1987).
[33] M. Alexe, V. Dragoi, M. Reiche, and U. Gosele, ''Low temperature GaAs/Si direct wafer bonding,'' Electron. Lett. **36**, 677–678 (2000).
[34] R. A. Grimm, ''Through-transmission infrared welding of polymers,'' Proceedings of the Society of Plastic Engineers Annual Technical Conference—ANTEC 1996, Indianapolis, IN, Vol. 1, pp. 1238–1244.
[35] H. Potente, J. Korte, and F. Becker, ''Laser transmission welding of thermoplastics: analysis of the heating phase,'' J. Reinf. Plast. Compos. **18**, 914–920 (1999).
[36] T. Ebert, ''Keeping a clear view joining transparent plastics by laser,'' Kunststoffe Plast. Europe **89**, 17–18 (1999).
[37] F. P. Incropera and D. P. DeWitt, *Fundamentals of Heat and Mass Transfer*, 4th ed. (Wiley, New York, 1996), pp. 236–240.
[38] P. Gravesen, J. Branebjerg, and O. S. Jensen, ''Microfluidics—a review,'' J. Micromech. Microeng. **3**, 168–182 (1993).
[39] S. Shoji and M. Esashi, ''Microflow devices and systems,'' J. Micromech. Microeng. **4**, 157–171 (1994).